Evaluation of installation timing of initial ground support for large-span tunnel in hard rock

Jimeng Feng[1], Congwen Yan[1], Lun Ye[1], Xiaoqi Ding[1], Junru Zhang[1], Zili Li[2]

1. School of Civil Engineering, Ssouthwest Jiaotong University, Chengdu, 610031, China

2. Civil & Environmental Engineering Building, School of Engineering, University College Cork, College Road, Cork, Republic of Ireland.

Corresponding author: Dr. Zili Li, zili.li@ucc.ie, +353 (0)21 490 2128

ABSTRACT:

In conventional drill and blast tunnelling, initial ground support is placed immediately after the current round is shot before excavation of the next round (i.e. one-round installation method). When tunnelling in hard rock, one-round installation of initial ground support conservatively ensures tunnel integrity, but meanwhile brings up other problems such as over-break at tunnel face, slow excavation rate and so forth. In this study, a large-span tunnel in Class Ⅲ hard rock was monitored by a network of sensors to investigate tunnel internal forces in three construction scenarios where initial ground supports were placed in different timing and sequence: 1) initial ground support installed immediately after current round 2) support installed after two rounds 3) support installed after three consecutive rounds. The collected field measurements together with construction records were evaluated from three aspects: structural stability, constructability and cost-effectiveness. Results show that the installation of initial ground support after two rounds generally led to the most regular and minimum tunnel internal forces of the three construction scenarios, whilst it managed to minimize under & over-break and allow more space for construction convenience. In the meanwhile, this installation sequence significantly accelerated tunnel advance rate at lower material cost.

Keywords: hard rock tunnelling, installation timing, constructability, initial ground support, large-span tunnel

1 INTRODUCTION

Rapid transportation development necessitates construction of a growing number of large-span tunnels to facilitate increasingly busy automobile travel in multi-lane highway network. Compared to traditional small single-lane road tunnels, a multi-lane highway tunnel requires much larger cross section with low height-span ratio, and therefore imposes greater challenges on drill & blast tunnel excavation (Sharifzadeh et al. 2013). The rigorous definition of large-span is inevitably subjective changing with time and varying from country to country. In general, the cross section of a large span road tunnel should be greater than 100 m^2 following International Tunnelling Association or 140 m^2 according to Japan Tunnelling Association Guan (2011).

Since 1980s, there have been an increasing number of large span road tunnels of more than 3 lanes built over the decades throughout the world. As a pioneer in late 20 century, trial construction was conducted in a tunnel of 3 lane dual carriage in New Tomei–Meishin expressway using TBM pilot tunnelling method (Miura et al., 2003). Due to increasing national traffic load, South Korea started to extend the existing 2-lane dual carriage highway road around Seoul to wider 4-lane dual carriage since the late 1980s, and has built a series of 4-lane large span road tunnels using New Austrian tunneling method (NATM). The first large-span tunnel of this Seoul project is Cheonggye Tunnel built in 1992 with a cross section of 186.42m^2, 19.68 m in width and 10.43 m in height, while the longest tunnel is Sapaesan Tunnel: 3.99 km in length, 19.69 m in width and 10.2 m in height (No et al., 2006). There are also some large underground tunnels built all over the world, including the Channel Tunnel between England and France with a cross section of 252 m^2 built in 2004, Prague Metro tunnel with a cross section of 220m^2 built in 2006 and etc. During the same

period, some large-span tunnels have been constructed in China as well: Dage mountain tunnel in Guizhou Province is the first large-span tunnel of two-lane dual carriage in China with a height of 18m and width of 22m; Longtou Mountain tunnel in the Ring Road Motorway of Guangzhou City is 13.6m in height and 21.6m in width, which was built in 2007 using double-sided drift excavation method and top heading excavation method. Since then, there have been some other representative large-span tunnel projects built in China over the decades such as Damao Mountain Tunnel in Xiamen City built in 2009, Jinji Mountain Tunnel in Fuzhou City built in 2015 and etc.

In practice, the large-span tunnels mentioned above were excavated using a variety of construction methods including Central Diaphragm (CD) method, double-sided drift excavation method, Tunnel Boring Machine (TBM) pilot tunnelling and etc., while the ground support system varies on a case by case basis, including a layer of initial ground support with two layers of secondary lining, two layers of initial support with high-strength secondary lining and high-strength initial support with a layer of secondary lining. According to incomplete statistics, there are only about 40 large-span tunnels all over the world up to date, to the authors' best knowledge, which is only as a small portion of total exiting tunnels, while the standard construction and design methods for large-span tunnel excavation have not yet been available.

One major concern for rock tunnelling is the installation timing of initial ground support to balance between tunnel structural performance and construction cost. Conventionally, the convergence-confinement method proposed by Pacher (1964) has been widely adopted in rock tunnel design as shown in Figure 1. This method considers the reduction of ground pressure in rock mass with increasing tunnel convergence (convergence-confinement curve) and therefore increasing load is then transferred to the tunnel support (support reaction line) (Oreste, 2009). As tunnel advances, the development of the tunnel radial convergence at a reference section can be graphically represented by a longitudinal displacement / deformation profile (LDP) (Gschwandtner et al., 2012; Paraskevopoulou et al., 2018; González-Cao et al., 2018). The rock tunnel stabilises when the convergence-confinement

curve and support reaction line intersect, indicating the optimal timing for secondary lining installation. In theory, the convergence-confinement curve and support reaction line may be determined by tunnel specifications and ground conditions, and as such that the installation timing of tunnel support and support stiffness enable the optimization of tunnel structural performance. In practice, one major difficulty of this method, however, is the determination of the convergence-confinement curve, which can hardly be formulated analytically to cater for a variety of different tunnelling conditions. Although some researchers (e.g. Zhang et al., 2017) attempted to propose approximate design formulas for optimal installation timing of tunnel support, the critical parameters in these formulas (e.g. convergence-time curve of surrounding rock) still relies on reliable field measurements. In addition, USACE (1997) summarised the rock-support interaction for the convergence-confinement method. That is, the ground can be generally classified into three categories: elastic stable, plastic stable ground and plastic unstable, whilst three categories of installation timing of ground support are early, on-time and delayed. The combination of ground relaxation and support timing & stiffness mainly determines the tunnel deformation (e.g. longitudinal displacement profile) and stability, which is also noted by Vlachopoulos et al. (2009) and González-Cao et al. (2018). In practice, the application of convergence-confinement method is affected by the tunnel depth and the tunnel transverse cross-section (Gonza´lez-Nicieza et al., 2008). In addition, the tunnel wall displacement and support load are a result of not only the tunnel advance excavation but also the time-dependent behaviour of the surrounding rock mass (Paraskevopoulou et al., 2018). Nevertheless, there was a lack of dedicated investigation on the effect of support installation timing particularly with little field data available to demonstrate or exemplify the proposed analytical rock-support interaction. In addition, the constructability and cost-effectiveness in relation to support installation timing was seldom discussed.

Besides formulated solutions, some other methods are also trialled to consider the optimal timing of ground support including experimental laboratory test and numerical simulation (Yang et al., 2008; Wang et al., 2010; Wu, 2011 and etc.). For example, Lai et al (2009)

116 conducted laboratory model scale test to investigate the effect of support installation timing
117 on tunnel behaviour in weak rock mass. The experimental test data demonstrated that the
118 optimisation of tunnel deformation allowance and installation timing of initial ground support
119 can effectively reduce the tunnel load. As an alternative, Su et al. (2015) developed both
120 two-dimensional and three-dimensional numerical models to evaluate the effect of the
121 installation timing of initial support on the stability of rock mass. The computed results
122 indicate that the optimal installation timing of initial ground support depends on the
123 displacement of surrounding rock mass as the tunnel advances. Up to date, there have been
124 some prediction / evaluation methods for initial support installation timing proposed available
125 in past studies, but their predicted tunnel behaviours (e.g. tunnel internal forces) are rarely
126 tested against field monitoring measurements on site, which on the contrary are rather
127 limited in literature. During drill & blasting tunnelling practice, the induced rock mass damage
128 and associated ground-tunnel interaction can hardly be represented realistically by those
129 methods discussed earlier due to complicated construction procedure, including (rock and
130 tunnel structure due to blasting, sequential excavation and etc., and as such the installation
131 timing of initial ground support in practice is still often determined by empirical visual
132 inspection rather than quantitative analysis.
133 In the interest of tunnel construction safety, majority of past studies focus on rock tunnelling
134 in weak rock, whereas little attention is paid on the support timing for tunnelling in hard rock.
135 It's usually not challenging for the installation of ground support for traditional small single-
136 lane tunnel construction in hard rock, provided that the rock mass is adequately self-
137 supporting after excavation. For a large-span tunnel of multiple lanes in hard rock, the big
138 tunnel cross section usually necessitates the installation of initial ground support at an
139 appropriate timing. Due to lack of experience and investigations, Standard and past
140 tunnelling practices of large-span in rock mass often excessively outweighs the structural
141 stability, but seldom analyses the tunnel constructability in limited underground space, tunnel
142 advance rate and other economic issues in a rational manner. In practice, the installation of
143 initial ground support immediately after the current round (i.e. one-round initial ground

support installation method) will limit the construction space between the excavation section at tunnel face and the following section for support installation; the insufficient construction space may lead to tunnel under & over-break, jeopardizing the construction rate and quality. Kolymbas (2005) pointed out that the installation timing of initial ground support should avoid large tunnel displacement and also allow sufficient construction space to enable efficient ground excavation. A balance between tunnel structural stability and construction cost for large-span tunnel excavation in hard rock is desired, whereas relevant literature is rather sparse.

This paper conducts a site investigation of a large-span tunnel construction project (i.e. JiangshuiQuan (JSQ) tunnel in China) in hard rock mass. To facilitate tunnel advance in a large-span tunnel, the tunnel crown centre section was excavated using double wedge cut excavation method together with millisecond blasting technology. In this project, three tunnel sections in the same Class III rock mass were constructed by different installation sequence of initial ground support. For each tunnel section, the tunnel structural performance was measured by a network of sensors, whilst construction records were analysed. Compared to conventional visible inspection method for determining the support installation timing, the field measurements in this investigation provides an opportunity to evaluate the effect of support installation timing on tunnel structural performance in a quantitative manner. The results show that among the three construction sequences, the installation of initial ground support after two rounds (i.e. two-round installation method) results in smallest tunnel internal forces and enables faster tunnel advance rate at lower material cost.

2 JIANGSHUIQUAN (JSQ) TUNNEL AND FIELD MONITORING

JiangshuiQuan (JSQ) tunnel near Ji'nan, Shangdong Province, China is so far the longest 4-lane dual carriage road tunnel in the world with a height-span ratio of 0.67 as shown in Figure 2: the tunnel is 3.1 km in length, 10.59m in height and 19.2m in width with a cross section area of 219.8m2. The rock mass along the tunnel route is classified into five different

classes according to basic quality (BQ) index in China standard (Highway tunnel design specification, 2004). The basic quality (BQ) of the rock mass is mainly determined by intact rock uniaxial compressive strength (UCS) and rock intactness index (K_V) for describing rock discontinuities. Another common rock mass classification scheme is international rock mass rating (RMR) developed by Bieniawski (1979), which takes uniaxial compressive strength of rock, rock quality designation (RQD), spacing of discontinuities, condition of discontinuities, groundwater condition and orientation of discontinuities into account, while the relationship between RMR and BQ rock mass classification scheme can be found the empirical equation below from Xu et al. (2014) and Yan et al. (2015):

$$BQ = 170 \ln \frac{15 + 0.24RMR}{5.7 - 0.06RMR} \quad (1)$$

The JSQ tunnel is embedded hard rock largely consisting of 14.5% Class V rock mass (BQ ≦ 250), 37.5% Class IV (251 ≦ BQ ≦ 350) and 48% Class Ⅲ ones (351 ≦ BQ ≦ 450); in relatively weak Class Ⅳ & V, tunnel face was partial exacted with side drift, while top heading was adopted in stiff and unweathered Class Ⅲ rock, where tunnel crown was excavated and lined with initial ground support before the construction of tunnel invert. The initial ground support consists of steel frames embedded in shotcrete, and a layer of reinforced cast-in-situ concrete is placed around the initial support thereafter as the secondary lining. The material properties of shotcrete, steel frame and reinforce concrete are given in Table 1.

2.1 TOP HEADING EXCAVATION AND BLASTHOLE CONFIGURATIONS

In this JSQ project, top heading in Class Ⅲ rock advances 3.5 meters per round, and field observation indicates consistent integrity and self-supporting capacity of rock mass after

197 excavation. The construction sequence of the top heading method for the large-span JSQ
198 tunnel is described as follows:
199
200 (1) Top heading and bench excavation
201 The tunnel crown at the tunnel face was excavated first before the bench as shown in Figure
202 3; for this large-span tunnel, the height of crown is between 7 ~ 9m, while the height of
203 bench is more than 4.5m. The typical interval between top tunnel face and bottom tunnel
204 face is around 20 meters depending on rock condition, tunnel support performance,
205 workmanship and etc. According to blasting method, the tunnel face may be generally
206 divided into 4 sections: crown centre section, crown contour, bench centre section, bench
207 contour, and their blasting methods are described as follows, respectively:
208
209 (2) Double wedge cut blasting method for tunnel crown centre section
210
211 Figure 4 shows the blasthole pattern of tunnel crown section excavated by double wedge cut
212 blasting method, where two cut blastholes (see ① in the figure) are symmetrically deployed
213 in a vertical wedge shape. The horizontal distance between the centreline of wedge cut
214 blastholes and tunnel centreline is 4.0 ~ 4.5m. The angle α between cut blastholes ①
215 and tunnel face ranges from 60 to 65 degree, whilst the angle β between helper cut
216 blastholes (see ② in the figure) and tunnel face ranges from 65 to 80 degree. At the sides of
217 wedge cut blastholes, helper blastholes (see ③ in the figure) were drilled perpendicular to
218 the tunnel face. Around the tunnel circumference, the bottom blastholes ④ and contour
219 blastholes ⑤ were drilled to the tunnel face with an inclination angle of 2 degree; the base of
220 contour blastholes ⑥ should penetrate outside of the tunnel circumference with a spacing
221 of 0.1m.
222
223 In this double wedge cut blasting method, the double wedge cut blastholes ① provide
224 sufficient space for blasting in subsequent blastholes (e.g. ② helper cut blasthole). The

detonation sequence of different blastholes is well controlled within millisecond levels, consisting of following steps: ① cut blastholes at tunnel sides → ② helper cut blastholes → ③ helper blastholes → ④ bottom blastholes → ⑤ contour blastholes, whilst the time delay between one step and the next should not be less than 50ms ~ 100ms. In practice, the adoption of double wedge cut method together with millisecond blasting technology improved the effectiveness of blastholes as to facilitate the tunnel advance per excavation round in a large-span tunnel.

(3) Shallow parallel hole cut blasting method for bench centre section

The bench centre section was excavated using common parallel hole cut blasting method in shallow depth. All the cut, helper and bottom blastholes are loaded by continuous charge method using No. 2 rock emulsion explosive with a dimension of φ 32mm × 300mm. At the back of each blasthole, delay electric detonator is placed for inverse initiation of explosives to minimize the danger of cutoff holes.

(4) Smooth blasting method for crown and bench contour

The tunnel crown and bench contour sections were excavated using standard smooth blasting method. Conventionally, the initial ground support is placed immediately after the current round is shot to ensure tunnelling stability. In practice, this one-round installation method, however, seriously impede drilling of blastholes in the next round, particularly, the contour blastholes around tunnel circumference. For example, Figure 5 illustrates the influence of initial support on blastholes drilling at the circumference. Due to the existence of the initial support, contour blastholes can hardly be drilled perpendicularly to the tunnel face (see Figure 5b) but at a certain angle of inclination (e.g. more than 2 degree) (see Figure 5a). Blasting in the inclined holes is more likely to cause ground over-break at the tunnel face than that in straight holes as shown in Figure 6. In this figure, the blastholes in round A

(marked by broken red lines) is rougher and more irregular than those in the next round B (marked by broken green lines); the drilling of the inclined blastholes in former A is due to the obstruction by the existing initial ground support (refer to Figure 5a), whereas the drilling of the straight blastholes in latter B is attainable without the obstruction (see Figure 5b). Compared to smooth tunnel circumference contour in round B, the ground over-break in round A due to the existence of initial support therefore cost additional shotcrete and construction time.

2.2 INSTALLATION TIMING OF INITIAL GROUND SUPPORT

In a large-span tunnelling project, one major concern is the timing of installation of initial ground support after blasting. In the interest of optimising tunnelling process without compromising tunnel stability, three construction methods of different support installation sequences were tested at three individual chainages of this project: 1) initial ground support installed immediately after current round (one-round installation) at chainage DK3+840 2) installed after two rounds (two-round installation) at chainage DK3+833 and 3) installed after three consecutive rounds (three-round installation) at chainage DK3+825. The three trialled tunnel chainages within a distance of 20 metres are embedded in the same ground conditions about 100 metres below the ground surface as shown in Figure 7: the upper part of the tunnel cross section is embedded moderately weathered grayish dolomitic limestone, whereas the lower part is in blue-gray limestone. The rock formations of these two layers of limestones are medium-thick laminated with slightly inclined beddings. Both of them are hard and well connected with no evidence of slaking. The Class Ⅲ hard rock properties are also confirmed by field and experimental lab test data as follows: elastic wave velocity u_p=3685m/s, unconfined compressive strength R_c=74.19Mpa, rock intactness index K_v=0.57 for lightly crushed rock, basic quality (BQ) =425. In addition, there are two main sets of joints developed in the rock mass with steep orientation and weak connections. The groundwater is karst water deep below the tunnel, and as such that the tunnel is usually damp but with no

visible water seepage except water dripping in rainy seasons.

For each construction method, a network of sensors was deployed in initial ground support as shown in Table 2 and Figure 8. Around the initial support circumference, 7 pairs of strain gauges were installed from sidewall to vault, which are numbered alphabetically from S-a to S-g in clockwise direction (see Figure 8a). At each location, strain gauges were placed in pair: one for intrados and the other for extrados to measure strains in shotcrete and steel frame. At the same 7 locations, earth pressure cells were installed to measure the total load acting on the initial support. Likewise, sensors were installed around the secondary lining at five locations (i.e. from S-A to S-G in Figure 8b) for strain measurement and pressure on the lining. Due to limited budget and allowable sensor installation time in this project, only secondary linings at chainage DK3+833 (two-round installation method) and chainage DK3+825 (three-round installation method) were instrumented with sensors but not for chainage DK3+840 (one-round installation method). This monitoring plan for secondary linings was confirmed by site engineers' field experience that in Class III hard rock the tunnel stability constructed by one-round installation method is usually guaranteed with more confidence than those by two-round or three-round installation methods.

In addition to tunnel structural monitoring, laser scanning was employed for surveying the under & over-break at the tunnel face for the three construction methods, whilst the construction cost and tunnel advancing rate were also well recorded. In the following sections, the analysis of field measurements and records will compare the three construction methods mainly from three aspects: tunnel structural stability, ground over-break and construction cost-effectiveness.

3 MONITORING RESULTS

In the analysis of tunnel structural stability, the field data of strain measurements and earth pressure evaluates the effect of the three different construction methods (i.e. one-round installation, two-round installation and three-round installation) on the tunnel structural behaviour. In this study, the field data in initial ground support is discussed first followed by the analysis of structural performance of secondary lining.

3.1 INITIAL GROUND SUPPORT

For the initial ground support, the sensor network recorded the development of the structural strain with time as tunnel advances, whilst the distribution of internal forces and earth pressure along the tunnel circumference 38 days after construction at the short-term steady state is then discussed. Although some field data was not available due to sensor damage during drill & blasting tunnel excavation, the collected field measurements still enable to reveal the general structural performance of initial ground support.

3.1.1 THE DEVELOPMENT OF INTERNAL FORCES

In this section, the strain measurements of initial ground support at different chainages are analysed, respectively: chainage DK3+840 for one-round installation, chainage DK3+833 for two-round installation and chainage DK3+825 for three-round installation. Figure 9 shows the strain development in shotcrete immediately after the construction of current round as the tunnel advances with time. Both the strain measurements in shotcrete extrados and intrados grow rapidly within about 10 days after the current round with the progressive hardening of shotcrete. The shotcrete stresses continue to build up gradually and sustain increasing earth pressure as the tunnel face advances further away, and then increase at a slower rate after 30 days. Similar trend is observed in the stress development in the steel frame with time as shown in Figure 10, suggesting the tunnel load stabilises gradually. The maximum compressive stress in shotcrete is 8.34 MPa, whilst the maximum compressive stress in steel frame is 125.7 MPa; both of them were within the allowable strength of material.

For two-round installation at chainage DK3+833, Figure 11 and 12 show the stress development of shotcrete and steel frame, respectively. Likewise, the stresses in these figures increase rapidly after the current round and then tend to converge after tens of days. At the short-term steady state, the stress magnitude induced by the two-round installation is generally smaller than that by one-round installation at chainage DK3+840: for example, the maximum compressive stresses of shotcrete and steel frame are 4.54 MPa and 117.8 MPa, respectively, both of which are smaller than the ones induced by one-round installation.

Figure 13 & 14 show the stress development of shotcrete and steel frame by three-round installation method at chainage DK3+825, respectively, which are both in line with those by one-round installation and two-round installation. In this condition, the maximum compressive stress of shotcrete is 9.4 MPa, which is the largest of the three installation methods. In particular, the compressive stress in steel frame builds up to 208.3 MPa, which equals to 88.6% of the yield stress of Q235 steel (i.e. 235 MPa). The stresses in steel frame due to three-round installation method are significantly greater than those by one-round and two-round methods, therefore posing a greatly higher risk of tunnel stability.

3.1.2 DISTRIBUTION OF INTERNAL FORCES AND EARTH PRESSURE

In this section, the stress measurements of shotcrete along the tunnel per unit length at the short-term steady state are converted to bending moment and axial forces, and their distributions around the tunnel circumference are plotted in Figure 15 a & b. Likewise, the stress measurements of steel frame are plotted in Figure 15 c & d.

In these figures, the internal forces distributions of one-round installation (DK3+840), two-round installation (DK3+833), three-round installation (DK3+825) are marked by green, red and blue lines with markers, respectively. For the shotcrete internal forces (Figure 15 c & d), both the one-round installation method and three-round installation method generate larger

and more irregular axial forces and bending moments around the tunnel crown than those by the two-round installation.

Compared to the one-round installation method, the installation of ground support after two rounds enables the development of ground arching more effectively in the rock mass around the tunnel, which carries more in-situ earth pressure and in turn leaves less load sustained by the initial tunnel ground support. As tunnel advances further away, the capability of ground arching may, however, degrade due to rock mass damage by drill & blasting if the tunnel opening is not supported several rounds after excavation. It is therefore that the rock mass excavated by three-round installation method can no longer sustain as much earth pressure as that by two-round installation method, and consequently the tunnel develops larger hoop thrust (axial forces) around.

In terms of the internal forces in the steel frames (Figure 15 c & d), the distributions of axial forces and moments for all the three installation methods are very irregular. In particular, the internal forces of tunnel structure excavated by three-round installation method are remarkable compared to the strength of the steel frame; the maximum axial forces of 589.2 kN at tunnel shoulder of three-round installation (DK3+825) is 88.6 % of the allowable strength of steel frame (613.4 kN). Likewise, the maximum bending moment 19.73 kN*m also occurs at chainage DK3+825 (three-round installation) as well, which is 60% of the allowable strength of steel frame (33.1 kN*m).

In addition, Figure 16 shows the earth pressure distribution around the tunnel circumference for the three installation methods. In general, the distribution of earth pressure at chainage DK3+840 (one-round installation) is the most irregular one with a maximum value of 62 kPa near the tunnel shoulder, followed by the relatively uniform pressure distribution in three-round installation, and then that of two-round installation with the minimum pressure. The findings of earth pressure distribution are generally in line with the distribution of internal forces of the three installation methods as described earlier.

As the tunnel is buried more than 100m in hard rock metres below the ground surface, the

majority of overburden (approximately 2000kPa = 100m tunnel depth x 20kN/m^3 soil & rock unit weight) is sustained by the ground arching whereas only a small fraction of less than 3.1% (smaller than 62kPa) is transferred to the initial ground support and tunnel structure. It is likely that the distribution of earth pressure and internal forces around the tunnel is due to local rock damage and stiffness degradation induced by drilling and blasting.

The internal force of tunnel structure is a governed by installation timing of tunnel support and rock stiffness degradation. If rock degradation is not considered, the latter the tunnel support is placed before rock yields or collapses, the more overburden will be sustained by ground arching with greater radial deformation (u) and in turn less tunnel support pressure (p_i) as shown earlier in Figure 1. In practice, the stiffness (D) of rock around unsupported tunnel opening reduces considerably due to drilling & blasting. Since the change of tunnel support pressure (Δp_i) is governed by the product of the change of tunnel radial deformation (Δu) and rock stiffness D, given the same incremental radial deformation (Δu), the smaller rock stiffness D due to drilling & blasting (e.g. two- or three- round installation method) will result in smaller reduction of tunnel support pressure (i.e. $\Delta p_{i,2}$ for two-round installation is smaller than $\Delta p_{i,1}$ for one-round installation) as shown in Figure 16; the solid green line represents the conventional ground response curve for one-round installation, the dotted red line stands for the ground response with a smaller rock stiffness due to drilling & blasting by two-round installation where the tunnel opening is not supported one round after excavation, and the long-dash-dot-dot blue line is then for three-round with an even smaller stiffness.

Likewise, the tunnel support curves (support reaction lines) differ for the three installation methods as shown in this figure. Given the same initial tunnel structure support property, the support curve of two-round installation (red dotted line) builds up with increasing tunnel radial deformation at a faster rate (slope θ_2 of the support curve) than that by one-round installation (green line slope θ_1); the smaller rock stiffness in two-round installation will result in relatively weaker ground arching and in turn more incremental tunnel structure reaction internal forces under the same incremental radial deformation. Nevertheless, the ultimate tunnel internal forces of two-round installation ($p_{i,2}$) can still be smaller than that of one-round

418 installation ($p_{i,1}$), as the initial tunnel support was placed latter. That is, the internal forces of
419 tunnel structure (i.e. tunnel support pressure p_i) are a combined result of installation timing of
420 tunnel support and rock stiffness degradation. Compared to two-round installation, the
421 reaction line of three-round installation starts latter at a greater radial deformation and builds
422 up at an even faster rate (blue line slope θ_3). The intersection with the three-round ground
423 response curve (i.e. the ultimate tunnel internal forces $p_{i,3}$) can be greater than that of two-
424 round installation ($p_{i,2}$).
425 In summary, Figure 16 shows the effect of installation timing on ground response curves and
426 tunnel structure forces in a qualitative manner, whereas the quantification of ground curve
427 requires more field measurements (e.g. the development of tunnel radial deformation and
428 convergence with time) and relevant case studies.
429

430 ## 3.2 SECONDARY LINING

431

432 Similar to the investigation of initial ground support, the development of secondary lining
433 structural performance during tunnel advance is analysed first, followed by the discussion on
434 the distribution of internal forces and earth pressure. Due to limited budget and installation
435 time, only two-round installation method and three-round installation were available for
436 sensor monitoring and comparison as described earlier. Unlike the sensor damage in the
437 initial ground support due to drill & blasting, almost all the sensors in the secondary lining
438 were working effectively during tunnelling, and as such the field strain measurements of
439 secondary lining are able to be converted to internal forces for better clarity.

440 ### 3.2.1 THE DEVELOPMENT OF INTERNAL FORCES

441
442 Figure 17 shows the development of axial force and bending moment with time at chainage
443 DK3+833 for two-round installation method. In this chainage, the axial forces around the
444 tunnel circumference are all in compression and increase at a similar rate.

445 In contrast, the axial forces induced by the three-round installation method varies
446 significantly around the tunnel circumference as shown in Figure 18. In particular, axial force
447 at the vault is in tension, which may cause cracks in concrete. Similar difference between
448 two-round installation method and three-round installation method can also be noted in the
449 stress development of embedded steel bar as shown in Figure 19; for two-round installation
450 method all the stresses in steel bar are in compression, whereas the steel bar stress at the
451 vault for three-round installation method is in tension. In these figures, the majority of curves
452 generally show stabilising trends with time beyond 25 ~ 30 days.
453
454
455

456 **3.2.2 DISTRIBUTION OF INTERNAL FORCES AND EARTH PRESSURE**
457

458 Figure 20 shows the distributions of internal forces in secondary lining for both two-round
459 installation method and three-round installation method. For two-round installation method
460 (red curve), the bending moment around the circumference is positive (intrados is in tension
461 and extrados is in compression) except the opposite negative moment at the vault. In
462 contrast, the negative bending for the three-round installation method occurs at the tunnel
463 side wall, whereas the remaining sections around the circumference are also under positive
464 moment. Regardless of different distribution of internal forces, the magnitude of internal
465 forces between the two installation methods are both not significant well within the
466 permissible envelope as shown in the moment-thrust diagram plotted in Figure 21.
467 In addition, Figure 22 compares the distribution of pressure acting on the secondary lining
468 between the two installation methods. The pressure in two-round installation method is
469 generally smaller and more uniform than that in three-round installation method, which is in
470 line with the structural performance of initial ground support.
471 In this case study, three installation timing methods of initial ground support was trialled for a

100m deep large-span tunnel in Class III rock mass, aiming to optimise tunnelling process and save construction cost without compromising tunnel stability. In general, the two-round or three-round installation methods may potentially be adoptable for large-span tunnelling in rock of similar class or even stiffer, largely depending on the ground response curves in the modified convergence-confinement method as shown in Figure 16b.

If the tunnel is excavated at a shallower depth within tens of metres, it is possible that the drilling & blasting has a significant impact on the rock stiffness around the unsupported tunnel opening and therefore much greater earth pressure may have to be sustained by initial ground support in two-round installation method than that of conventional one-round installation. In addition, the tunnelling-induced settlement near the ground surface may also be a concern. On the contrary, if tunnelling at the depth of hundreds of metres, the deeper the tunnel is, the less challenging the construction generally would be, until down to over 400m, where rock burst and some other problems may be encountered.

4 CONSTRUCTABILITY AND ECONIMCAL ASPECT

Blasting in rock tunnelling usually induces under & over-break at tunnel face. In practice, the amount of over-break areas and average linear over-break, which is defined as over-break areas normalised by arch length, are two vital parameters for tunnel construction quality control. Figure 23 compares the amount of over-break and average linear over-break by the three installation methods. As mentioned earlier, the one-round installation of initial support obstructs the drilling process and hence generates the greatest over-break around tunnel circumference, followed by two-round installation and then the three-round installation where more spaces are available at tunnel face for efficient construction. In addition, Figure 24 shows the laser scanning contours around the tunnel circumference at DK3+840 and DK3+825. The one-round installation method (DK3+840) creates much more irregular tunnel circumference contour with greater over-excavation areas than those by three-round

installation method (DK3+825), as expected.

The installation of initial support after two or three rounds facilitates tunnel construction in different rounds and therefore generates smoother tunnel circumference after blasting than that by one-round installation method and effectively saves shotcrete cost. Compared to one-round installation, the two-round installation method saves about 9m^3 of shotcrete per round for each 3.5m tunnel advance at a construction rate of 125m per month 31.6% faster than that of 95m per month by the one-round installation method. Table 3 shows the average time duration per tunnel excavation round (3.5m tunnel advance) for all the three installation methods based upon construction records. One-round installation method costs the longest time per tunnel advance, as it requires more complicated construction procedures, including drilling of blastholes, charging / loading, spraying shotcrete and etc., for each individual excavation round due to the obstruction by the existing initial ground support in the last round. On the other hand, the three-round installation method saves some time for drilling and charging, but much more time has to be spent on safety provisions as to ensure tunnel stability before the start of next round. On average, the two-round installation method cost minimal time of the three trialled methods; it saves 28% construction time than conventional one-round method.

In summary, the two-round installation method generally results in the smallest tunnel internal forces with the optimal stability of the three trialled methods, whilst it significantly saves the construction cost, duration and accelerates tunnel advance rate when compared to the conventional one-round installation method.

5 CONCLUSION

Unlike most past research focusing on tunnelling safety in weak rock, this study instead investigates a large-span tunnel excavation project in Class III hard rock. In this project, three different construction sequences of initial ground support were trialled as to evaluate the effect of the installation timing on tunnel structural performance, constructability and

other economic aspects. A network of sensors was deployed on both initial ground support and secondary tunnel lining to monitor the tunnel structural performance due to these three installation methods. The main findings from the analysis of field measurements of tunnel structure together with construction records on site are listed as the below:

- In this tunnelling project, two main blastholes were cut in a vertical wedge shape and denoted together with millisecond blasting technology for top heading excavation in tunnel crown centre section. This double wedge cut method managed to improve the effectiveness of blastholes in a large-span tunnel and therefore facilitated the tunnel advance per excavation round.
- In conventional analysis of ground-tunnel interaction, the later the initial support is placed, the smaller earth pressure acting on tunnel structure as ground arching usually sustains more ground load before rock failure. In contrast, this tunnelling project in Class III hard rock addressed that the internal forces of tunnel structure (i.e. tunnel support pressure p_i) are a combined result of installation timing of tunnel support and rock stiffness degradation due to drilling & blasting.
- Among the three construction sequences trialled in this study, the installation of initial ground support after two rounds (two-round installation method) enables the development of ground arching for tunnel structural stability before rock mass degrades or fails due to subsequent tunnel excavation. Field measurements of the three construction sequences indicate that the two-round installation method results in the smallest and most uniform load acting on tunnel, and therefore generally smallest internal forces in both the initial ground support and secondary lining of the three installation methods.
- In particular, the maximum internal forces of initial ground support induced by three-round installation method built up to 88.6 % of the allowable strength of steel frame, posing a significantly higher risk of tunnel stability. Field observations of damaged

554 rock mass and overly-excavated tunnel circumference suggest that the drilling &
555 blasting during the three-round tunnelling process may overly reduce the ground
556 stiffness and arching capability, which in turn leaves more remaining earth pressure
557 sustained by tunnel structure.
558 • Laser scanning at tunnel face indicates that the one-round installation of initial
559 support leads to greatest over-break around tunnel circumference, followed by two-
560 round installation and then the installation of initial ground support after three
561 consecutive rounds (three-round installation). Besides, the one-round installation
562 method creates more irregular and rougher tunnel circumference than that excavated
563 by two-round or three-round installation methods. In practice, control of over-break by
564 two-round and three-round installation methods substantially saves the cost of
565 shotcrete and time for initial support construction.
566 • Compared to one-round installation of initial support, the installation of initial ground
567 support after two or three rounds allows more operation space near tunnel face to
568 facilitate drilling and construction process. In particular, the optimisation of
569 constructability by two-round installation in this project effectively accelerate tunnel
570 advance rate without compromising tunnel safety.
571
572 Admittedly, excavation safety and structural performance certainly prioritise in a
573 tunnelling project, whilst constructability, cost-effectiveness and other issues should also
574 be carefully analysed if structural stability is not compromised. The comparison of two-
575 round and three-round installation methods against conventional one-round installation in
576 this study provides some reference of alternative construction sequences for large-span
577 tunnel construction in hard rock. In general, two-round installation method is likely to
578 bring more economic benefits (e.g. lower construction cost and faster tunnel advance
579 rate) than that by conventional one-round method for tunnel excavation in Class III hard
580 rock mass whilst at a lower risk of tunnel stability. Future study may further investigate
581 the installation timing of initial ground support in hard rock including more large-span

tunnelling cases, aiming to provide a generic and broadly-applicable guidance for tunnelling industry. In practice, ground uncertainties and tunnelling specifications differ from one project to another. It is the responsibility of tunnel stakeholders to balance structural stability and economic issues to maximise the impact on society at favourable cost under the guidance of wise engineering judgement.

6 ACKNOWLEDGEMENT

This research is sponsored by the National Natural Science Foundation of China (No. 51508476). In particular, the assistance from China Tiesiju Civil Engineering Group for field monitoring in Jiangshuiquan (JSQ) tunnel is gratefully acknowledged.

REFERENCES

Bieniawski, Z. T., 1979. The Geomechanics Classification in Rock Engineering Applications, Proceedings, 4th International Congress on Rock Mechanics, ISRM, Montreux. A. A. Ballkema, Rotterdam, 2, pp. 41-48

Highway tunnel design specification, (JTG D70-2004), 2004. People's Republic of China industry standards. China Communication Press. (in Chinese)

González-Cao, J., Alejano, L.R., Alonso, E., Bastante, F.G., 2018. Convergence-confinement curve analysis of excavation stress and strain resulting from blast-induced damage, Tunnelling and Underground Space Technology, 73, pp. 162–169.

Gonza´lez-Nicieza, C., Alvarez-Vigil, A.E., Menendez-Dıaz, A., Gonza´lez-Palacio, C., 2008. Influence of the depth and shape of a tunnel in the application of the convergence–confinement method, Tunnelling and Underground Space Technology, 23, pp. 25-37.

Gschwandtner, G., Galler, R., 2012, Input to the application of the convergence confinement method with time-dependent material behaviour of the support, Tunnelling and Underground Space Technology, 27, pp. 13-22.

Guan, B., 2011. Collection of key points in construction of tunnel project (second edition) [M]. China Communications Press, Beijing, China

Kolymbas, D., 2005. Tunnelling and Tunnel Mechanics A Rational Approach to Tunnelling, Springer, Germany

Lai, H., Lin Y., Xie, Y., Yang, X., 2009. Influence of supporting opportunity on stress characteristics of soft-weak surrounding rocks in highway tunnels. Chinese Journal of Geotechnical Engineering, 31, pp. 390-395. (in Chinese)

Miuraa, K., Yagib, H., Shiromac, H., Takekunid, K., 2003. Study on design and construction method for the New Tomei–Meishin expressway tunnels, Tunnelling and Underground Space Technology 18, pp. 271–281

No, S., Noh, S., Lee, S., Seo, J., 2006. Construction of long and large twin tube tunnel in Korea–Sapaesan tunnel. Tunnelling and Underground Space Technology, 21(3), pp. 393

Oreste, P., 2009. The Convergence-Confinement Method: Roles and Limits in Modern Geomechanical Tunnel Design, American Journal of Applied Sciences, 6 (4), pp. 757-771

Pacher, F., 1964. Deformations messungen in Versuchsstollen als Mittel zur Erfoschung des Gebirgs verhaltens und zur Bemessung des Ausbaues. Felsmechanik und Ingenieursgeologie，Supple- mentum IV. (in German)

Paraskevopoulou, C., Diederichs, M., 2018. Analysis of time-dependent deformation in tunnels using the Convergence-Confinement Method, Tunnelling and Underground Space Technology, 71, pp. 62–80.

630 Sharifzadeh, M., Kolivand, F., Ghorbani, M., Yasrobi, S., 2013. Design of sequential
631 excavation method for large span urban tunnels in soft ground – Niayesh tunnel,
632 Tunnelling and Underground Space Technology, 35, pp. 178–188
633 Su, K., Cui, J., Zhang, Z., 2015. Method of choosing initial supporting time during tunnel
634 excavations. Journal of Central South University (Science and Technology), 46(08),
635 pp. 3075-3082. (in Chinese)
636 United States Army Corps of Engineers (USACE), 1997. Engineering and Design
637 Tunnels and Shafts in Rock EM 1110-2-2901, Department of the Army,
638 Washington, DC, USA.
639 Vlachopoulos, N., Diederichs, M. S., 2009. Improved Longitudinal Displacement Profiles
640 for Convergence Confinement Analysis of Deep Tunnels, Rock Mechanics Rock
641 Engineering 42, pp. 131–146.
642 Wang, Z., Fang, J., Xia, C., Bian, Y., Jin, L., 2010. Determination method of supporting
643 time for secondary lining in tunnel considering rock creep behaviors. Chinese
644 Journal of Rock Mechanics and Engineering, 29(S1), pp. 3241-3246. (in Chinese)
645 Wu, M., 2011. Study on the space-time effect of large span flat arch tunnel and the
646 optimal timing of secondary lining. PhD thesis, Chongqing University, (in Chinese)
647 Xu, H., Chen, F., Wang, B., Hua, Z., Geng, H., 2014. Relationships between RMR and
648 BQ for rock mass classification and estimation of its mechanical parameters,
649 Chinese Journal of Geotechnical Engineering, 36(1), pp. 195-198, (in Chinese)
650 Yang, J., Chen, W., Guo, X., 2008. Effect of supporting time on stability of small spacing
651 roadway tunnel. Rock and Soil Mechanics, 02, pp. 483-490. (in Chinese)
652 Yan, R., Shen, Y., 2015. Correlation of Revised BQ System in China and the
653 International Rock Mass Classification Systems, Journal of Civil Engineering
654 Research, 5(2) pp. 33-38

655 Zhang, J., Wang, R., Zhou, Z., Zheng, L., Zhang, R., Wang, L., Xie, H., 2017. Optimum
656 support time of brittle underground cavern based on time-dependent deformation.
657 Chinese Journal of Geotechnical Engineering, 39(10) pp. 1908-1914. (in Chinese)

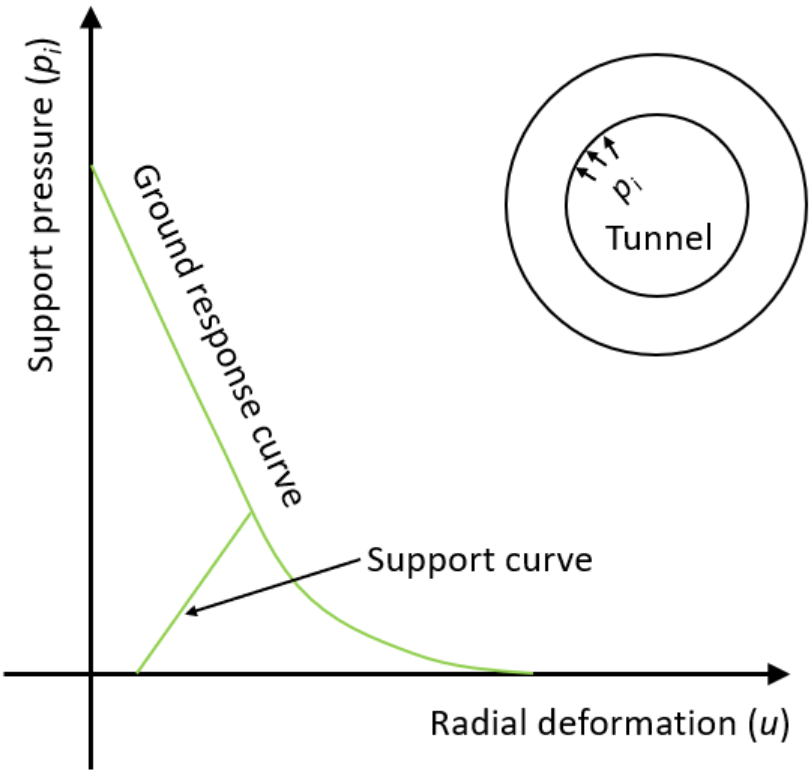

Fig.1 Ground and support response curves (reedited based upon Pacher (1964))

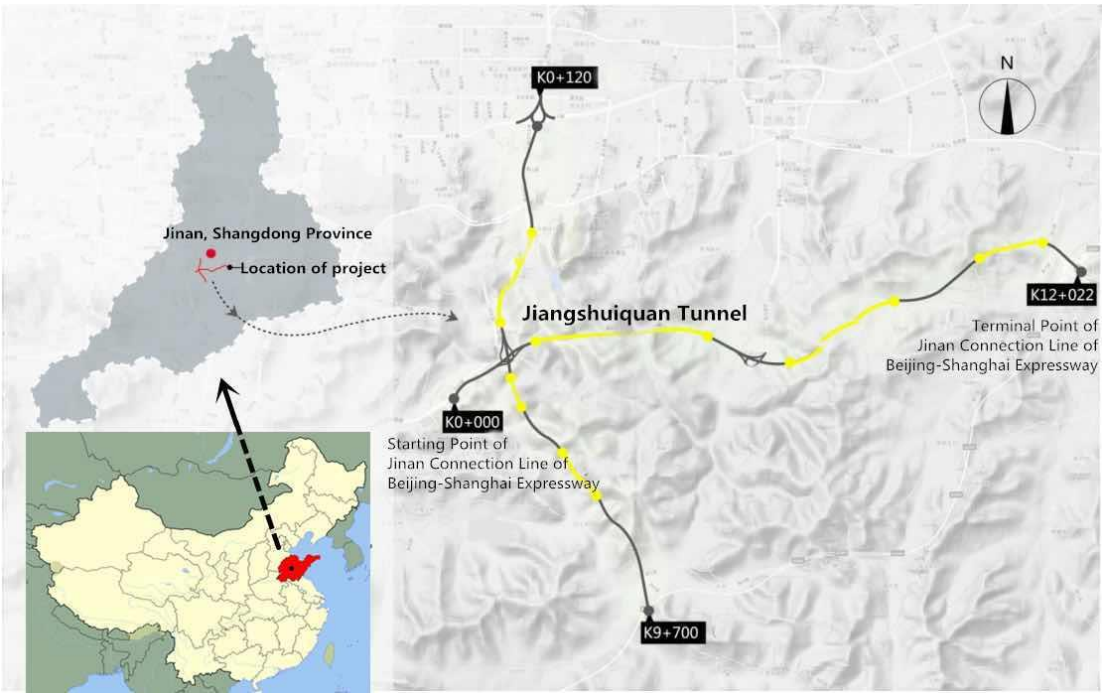

(a) Location and plane layout of JiangshuiQuan (JSQ) tunnel

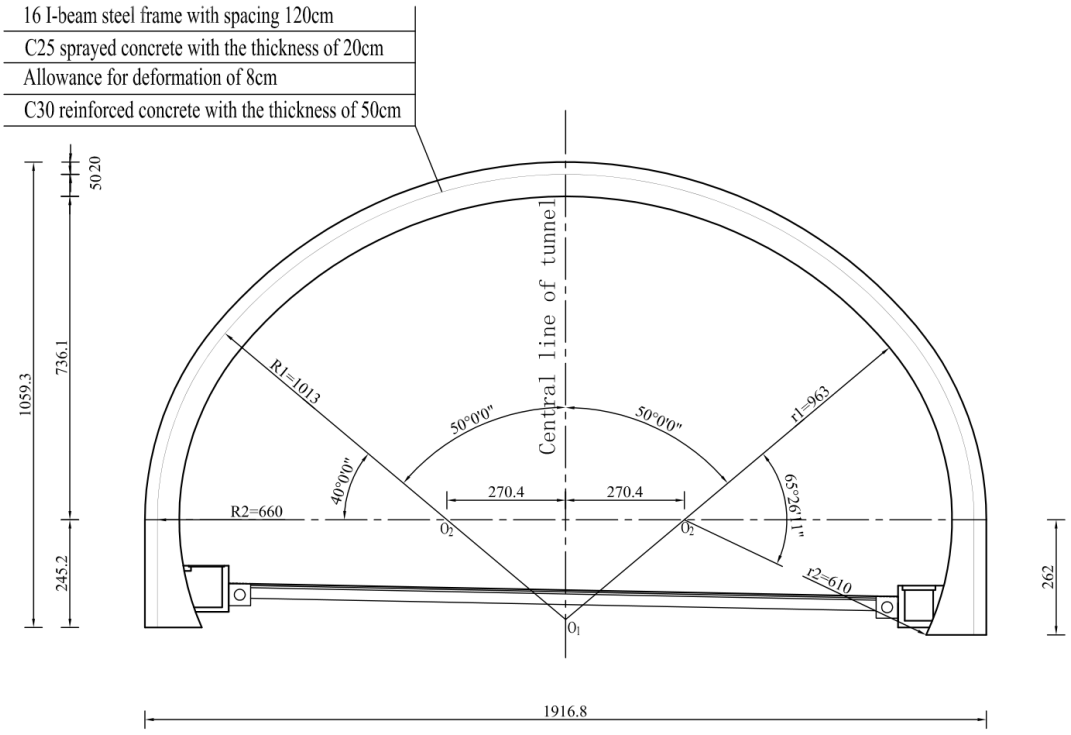

(b) Design of the transverse tunnel cross section (unit: cm)

Figure 2 Overview of JSQ tunnel project

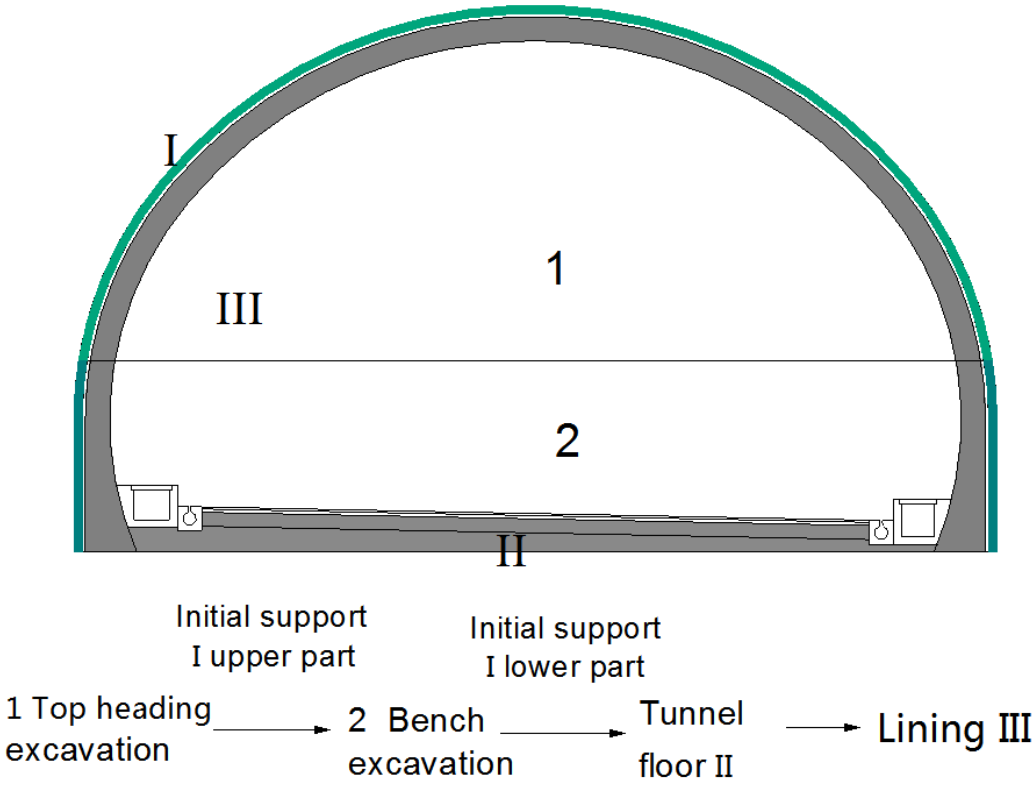

(a) Front view

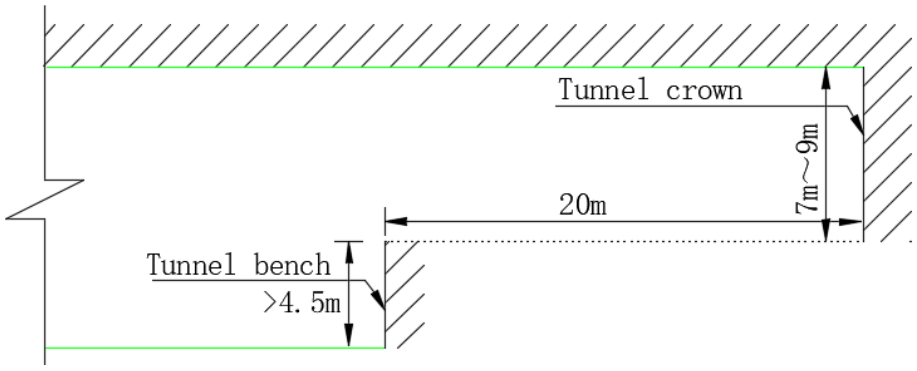

(b) Side view

Fig.3 Top heading construction method in Class III surrounding rock

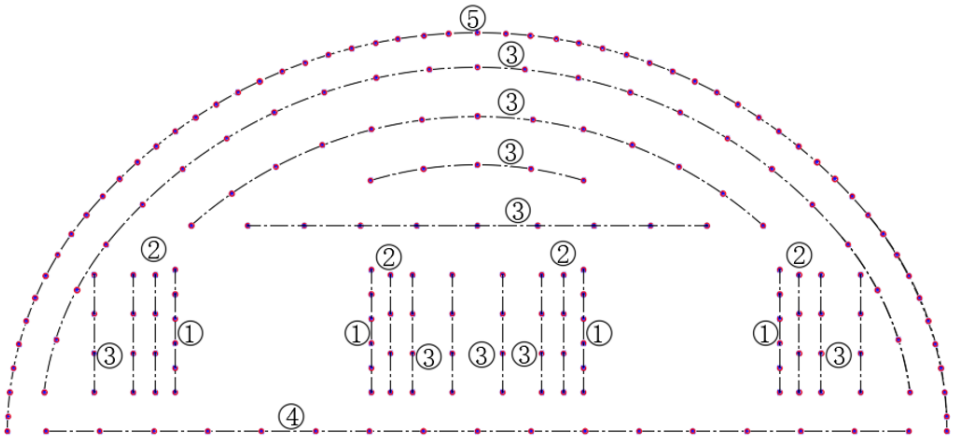

(a) Front view

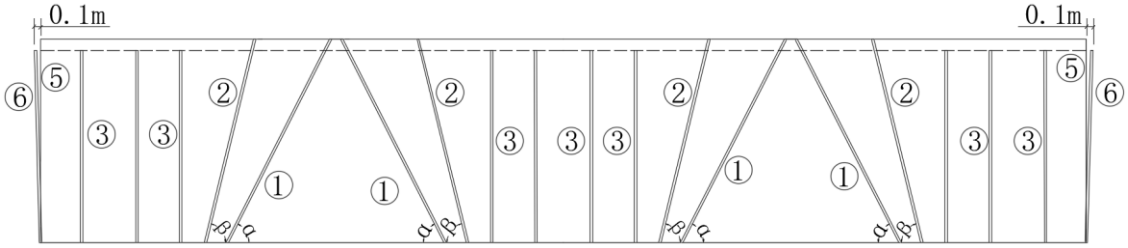

(b) Top view

Figure 4 blasthole pattern design for tunnel crown excavation

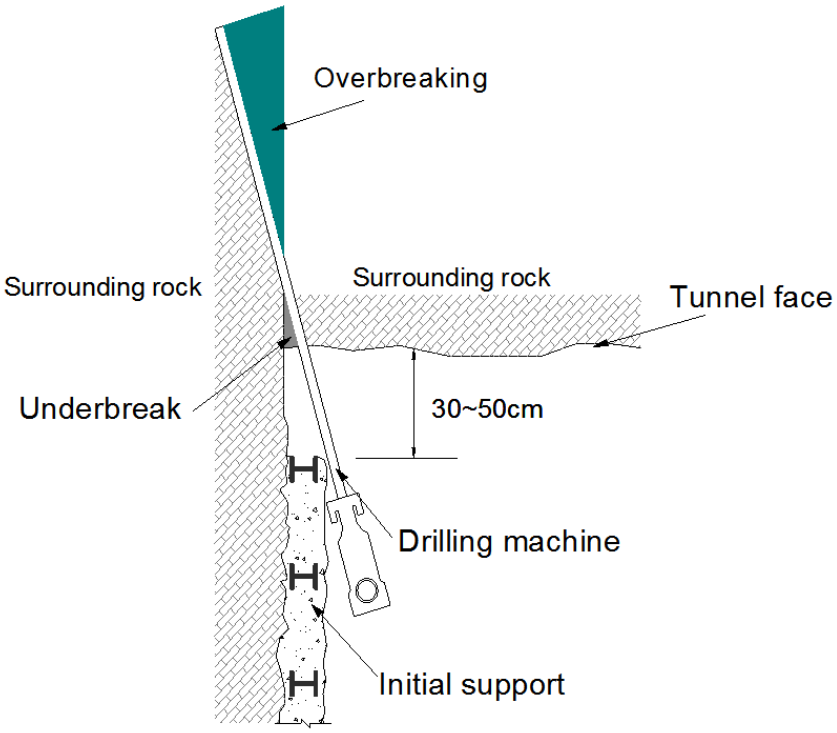

(a) Immediate installation of initial support after the current round (one-round installation)

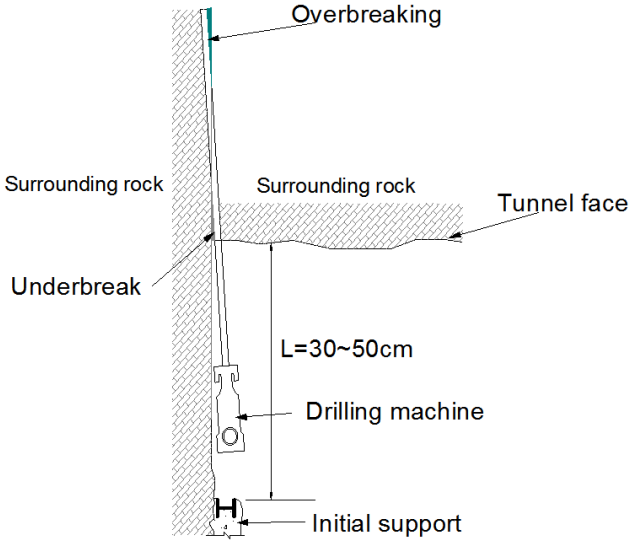

(b) installation of initial support after two rounds (two-round installation)

Fig.5 Schematic of contour balsthole drilling (Top view)

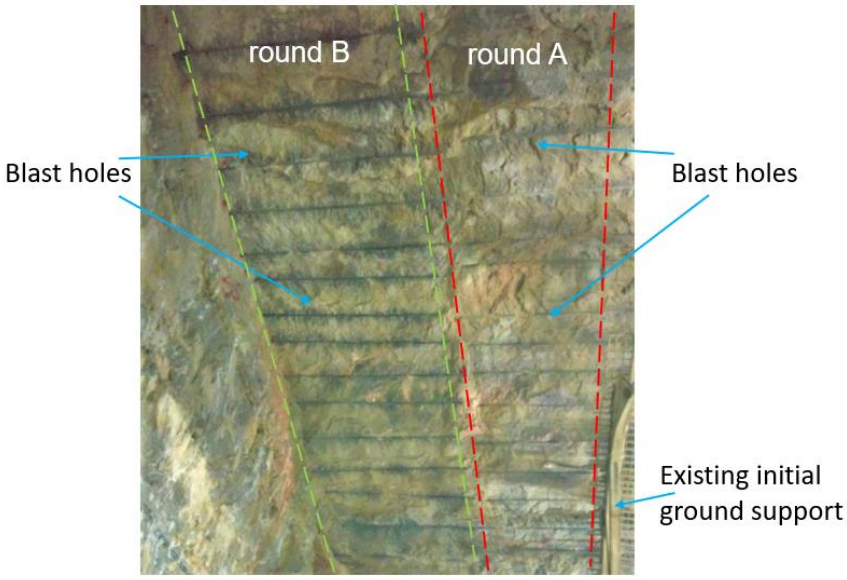

Fig.6 Blast holes in the arch after blasting

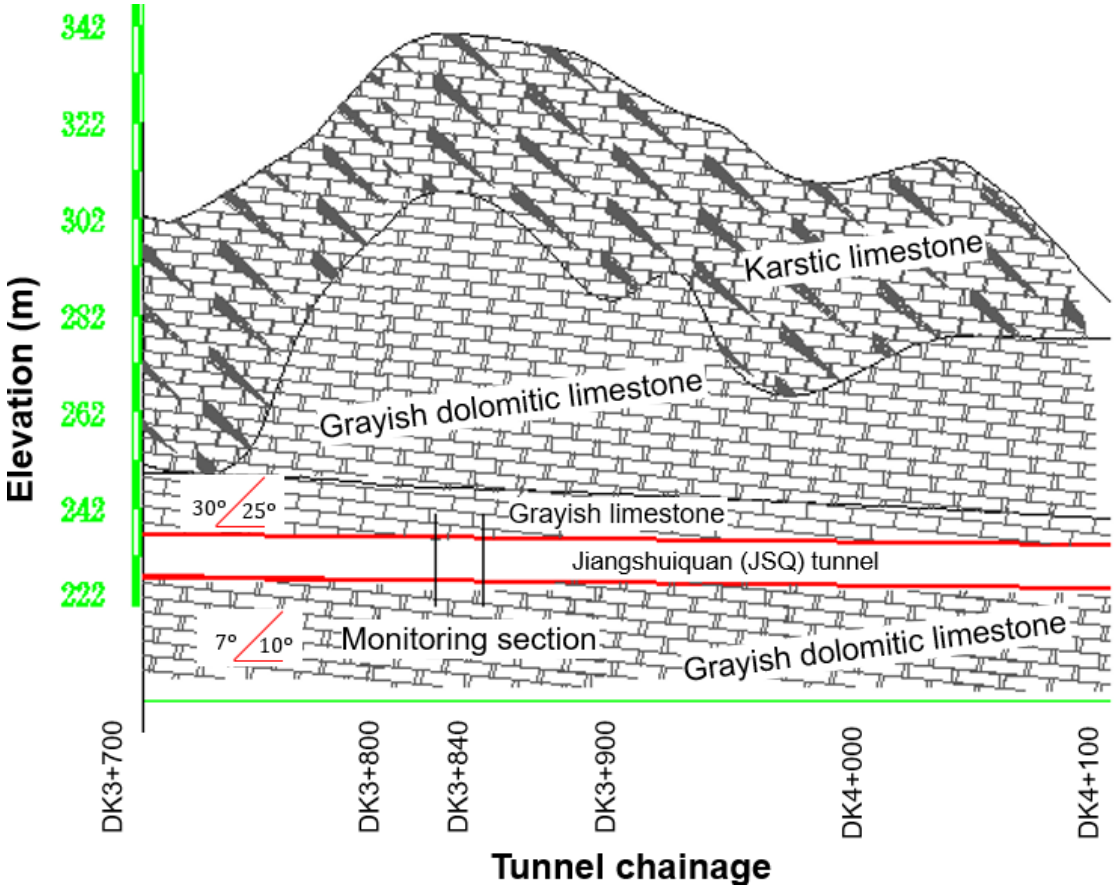

Figure 7 Geological condition of the monitoring section in Jiangshuiquan (JSQ) tunnel

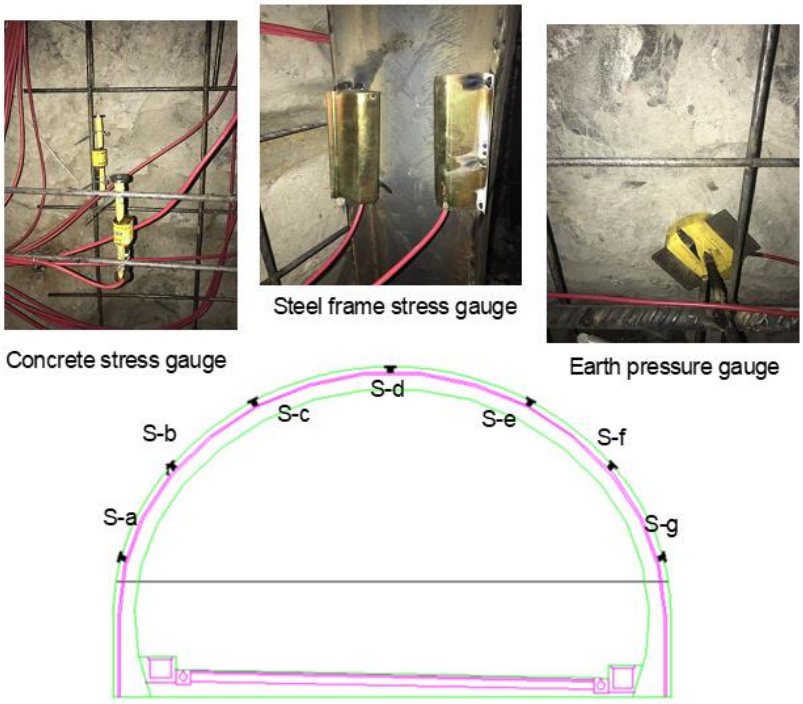

(a) initial ground support

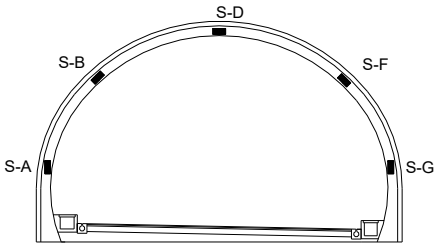

(b) secondary lining

Fig.8 Sensor deployment on site

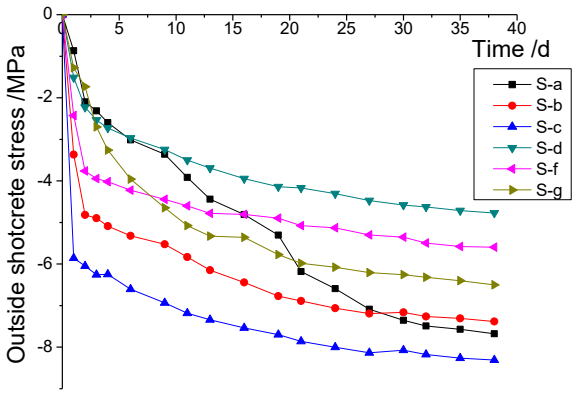

(a) near shotcrete extrados

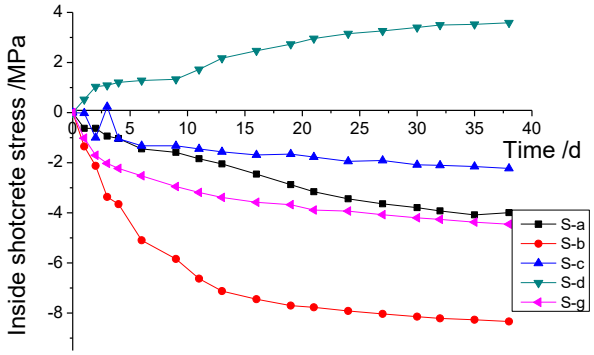

(b) near shotcrete intrados

Fig.9 The stress development in shotcrete at Section 840 for one-round installation method

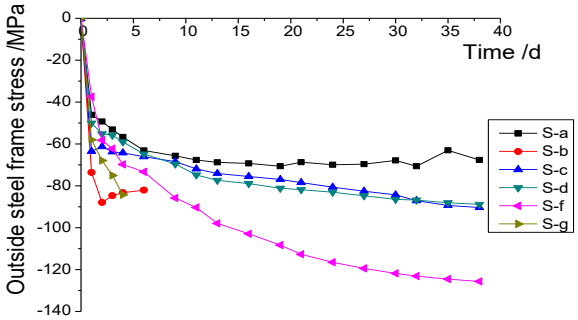

(a) in steel frame extrados

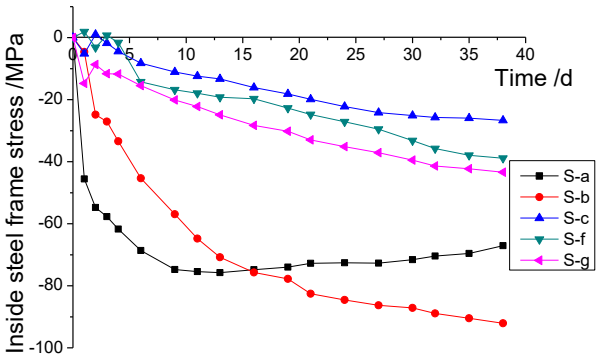

(b) in steel frame intrados

Fig.10 The stress development in steel frame at Section 840 for one-round installation method

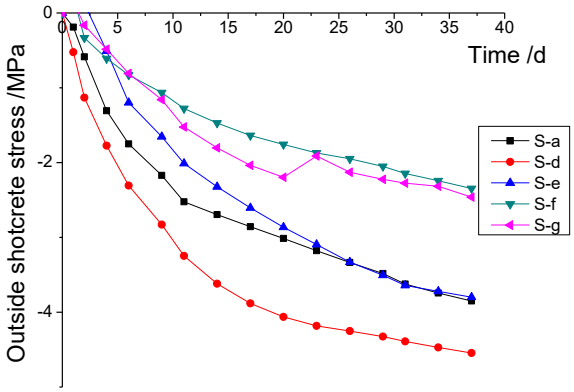

(a) near shotcrete extrados

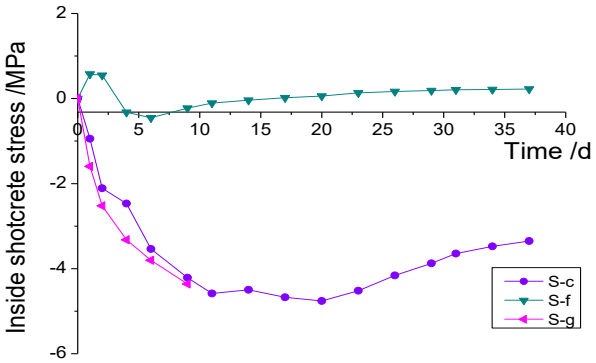

(b) near shotcrete intrados

Fig.11 The stress development in shotcrete at Section 833 for two-round installation method

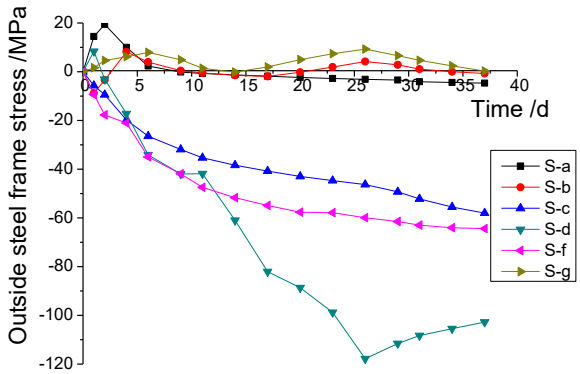

(a) in steel frame extrados

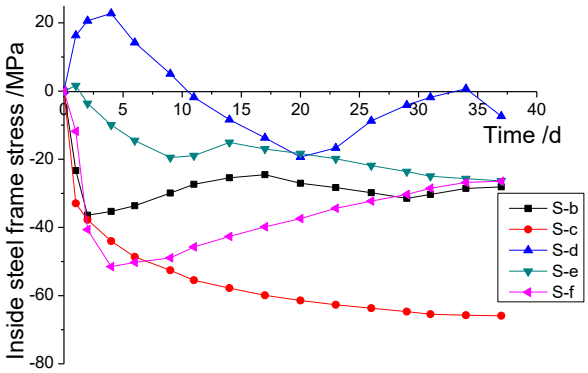

(b) in steel frame intrados

Fig.12 The stress development in steel frame at Section 833 for two-round installation method

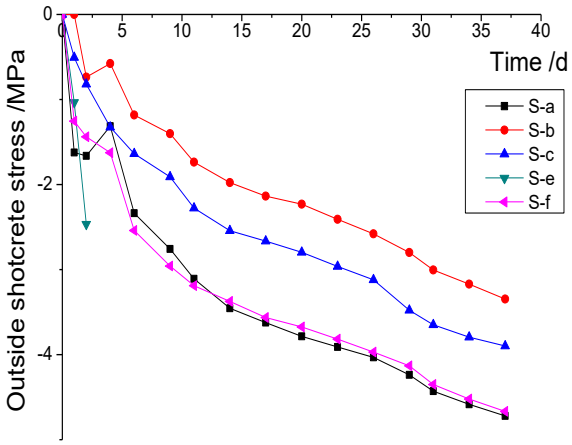

(a) near shotcrete extrados

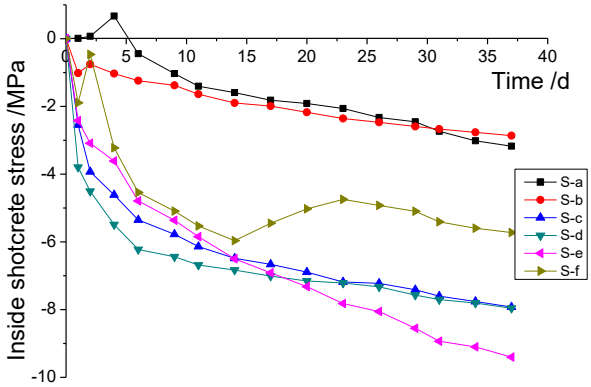

(b) near shotcrete intrados

Fig.13 The stress development in shotcrete at Section 825 for three-round installation method

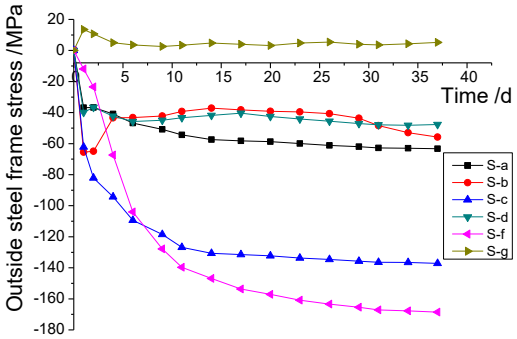

(a) in steel frame extrados

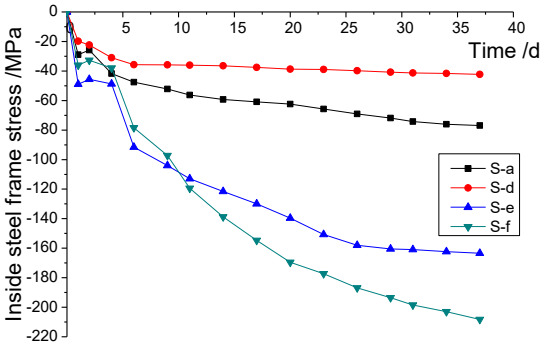

(b) in steel frame intrados

Fig.14 The stress development in steel frame at Section 825 for three-round installation method

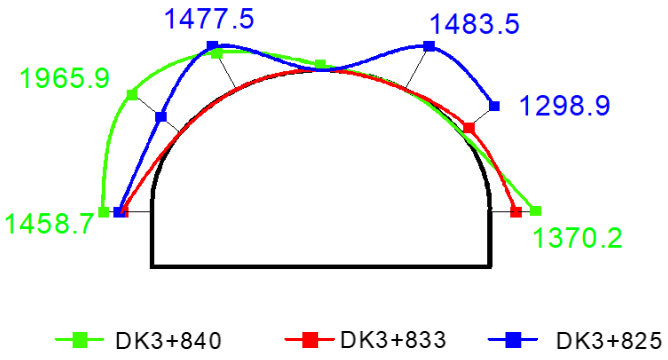

(a) Axial force of shotcrete /kN

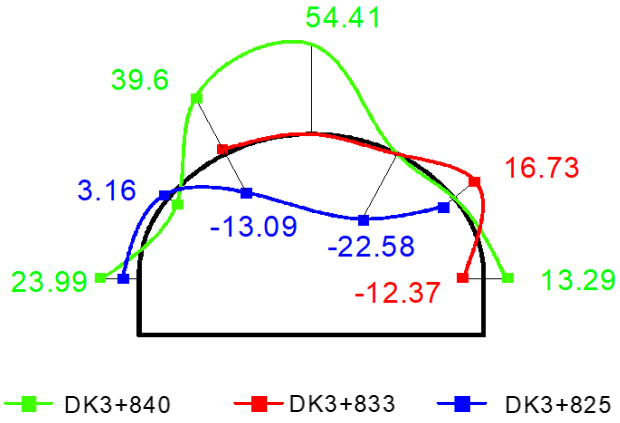

(b) Moment of shotcrete /kN m

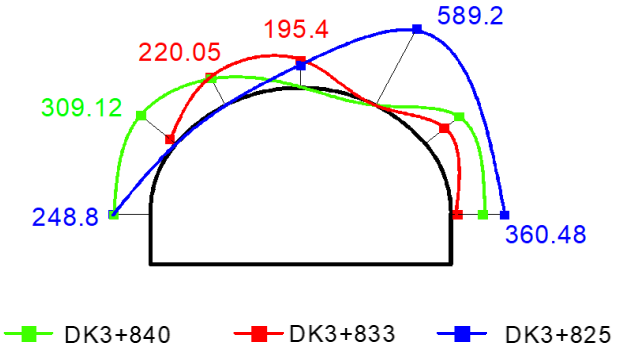

(c) Axial force of steel frame /kN

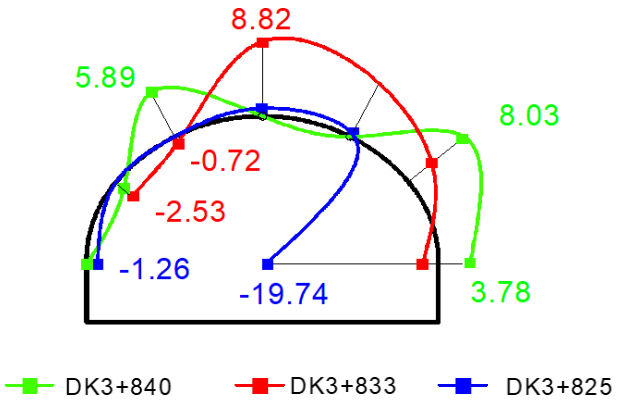

(d) Moment of steel frame /kN m

Fig.15 Internal force diagrams of initial ground support (green line of one-round installation (DK3+840), red line for two-round installation (DK3+833) and blue line for three-round installation (DK3+825))

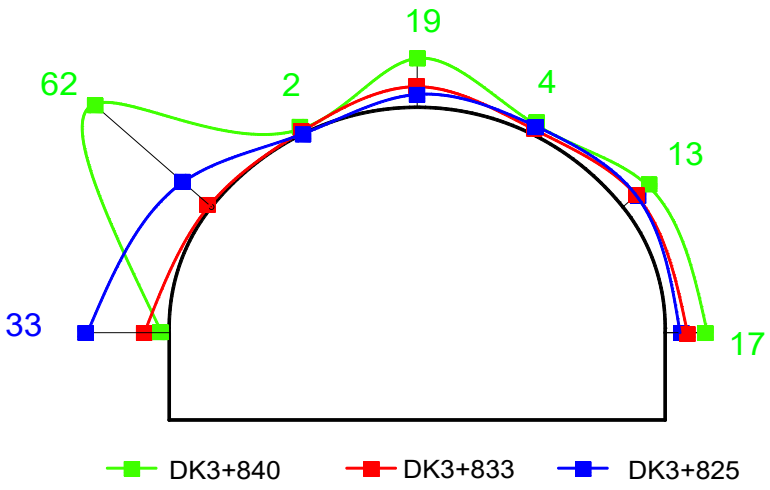

(a) surrounding rock pressure on initial ground support /kPa

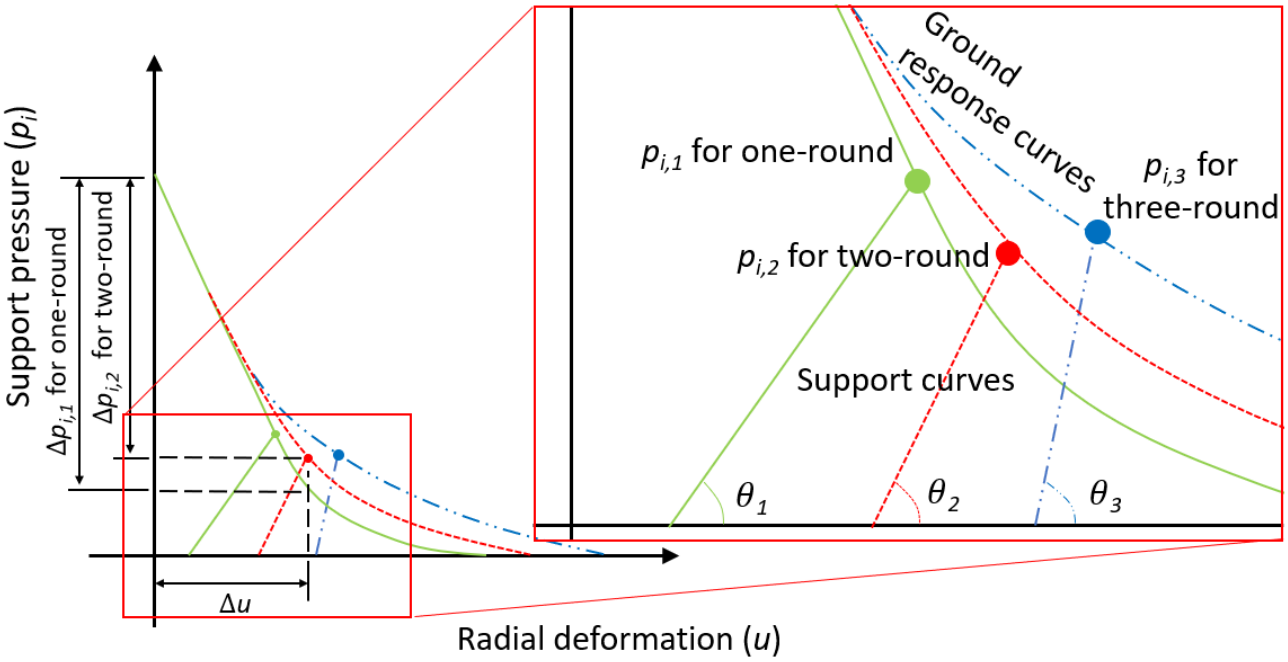

(b) The modified ground and support response curves

Figure 16 the effect of installation timing on the initial support pressure (green line of one-round installation (DK3+840), red line for two-round installation (DK3+833) and blue line for three-round installation (DK3+825))

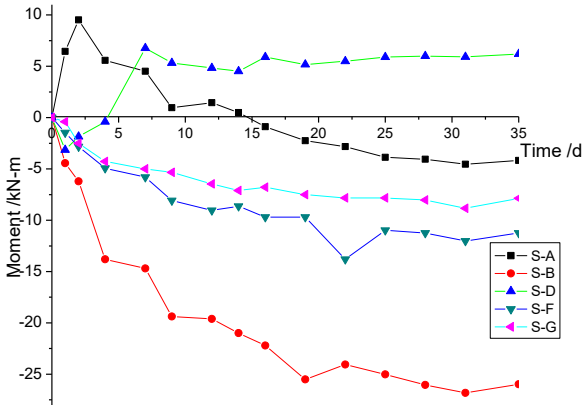

(a) Secondary lining moment

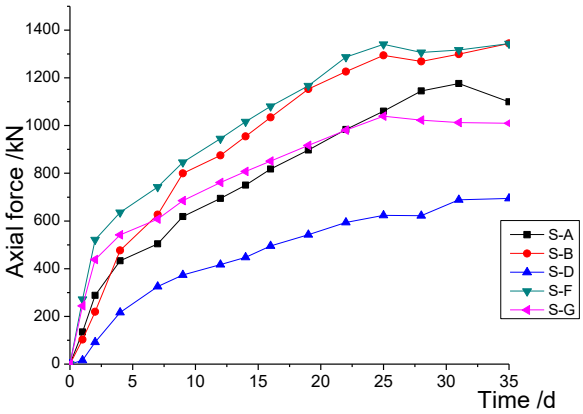

(b) Secondary lining axial force

Figure 17 Internal forces of secondary lining at Section 833 for two-round installation method

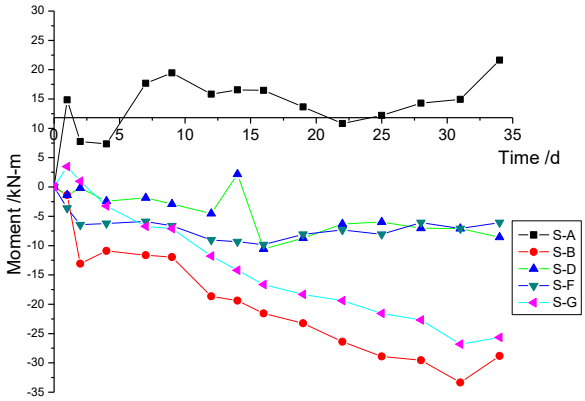

(a) Secondary lining moment

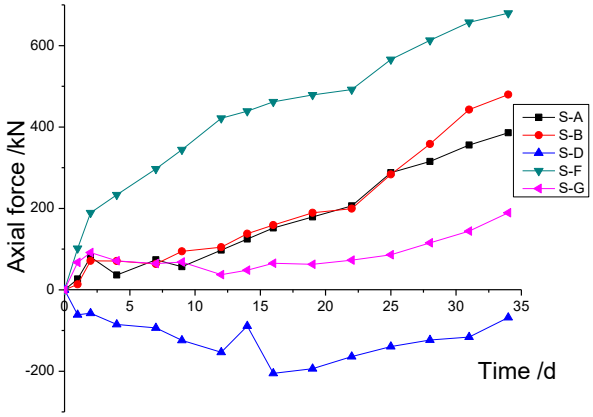

(b) Secondary lining axial force

Figure 18 Internal forces of secondary lining at Section 825 for three-round installation method

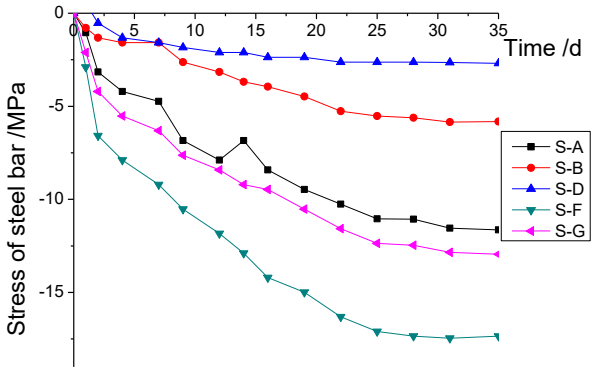

(a) Stress of steel bar at Section 833 for two-round installation method

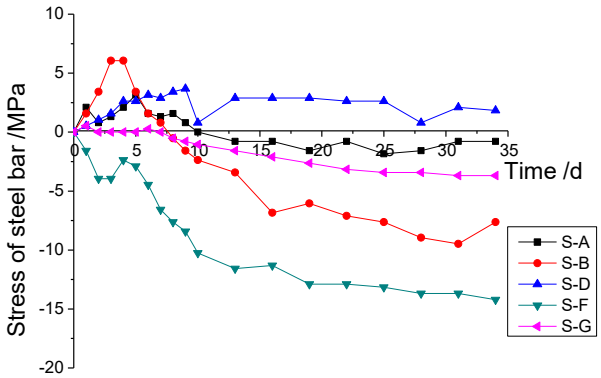

(b) Stress of steel bar at Section 825 for three-round installation method

Fig.19 The stress development in steel frame in secondary tunnel lining

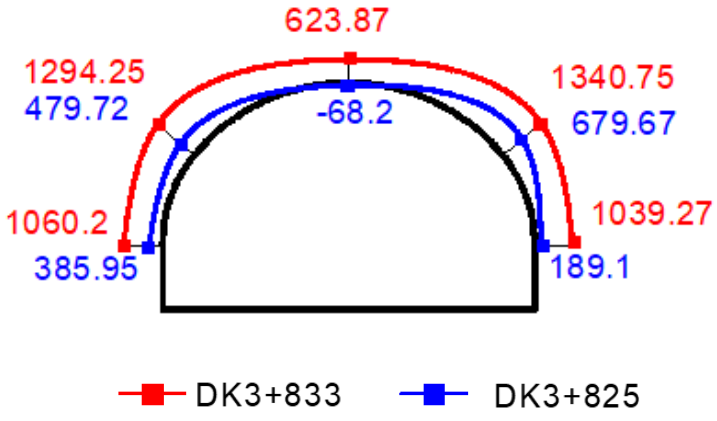

(a) Axial force of shotcrete /kN m

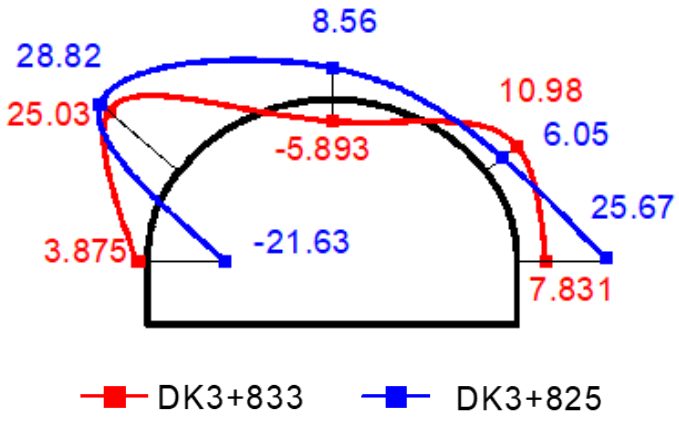

(b) Moment of shotcrete /kN m

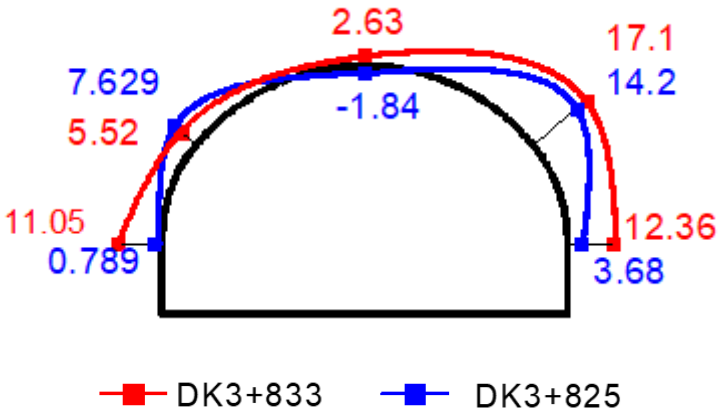

(d) Axial force of steel bar /kN

Fig.20 Internal force and pressure on secondary lining (red line for two-round installation (DK3+833) and blue line for three-round installation (DK3+825))

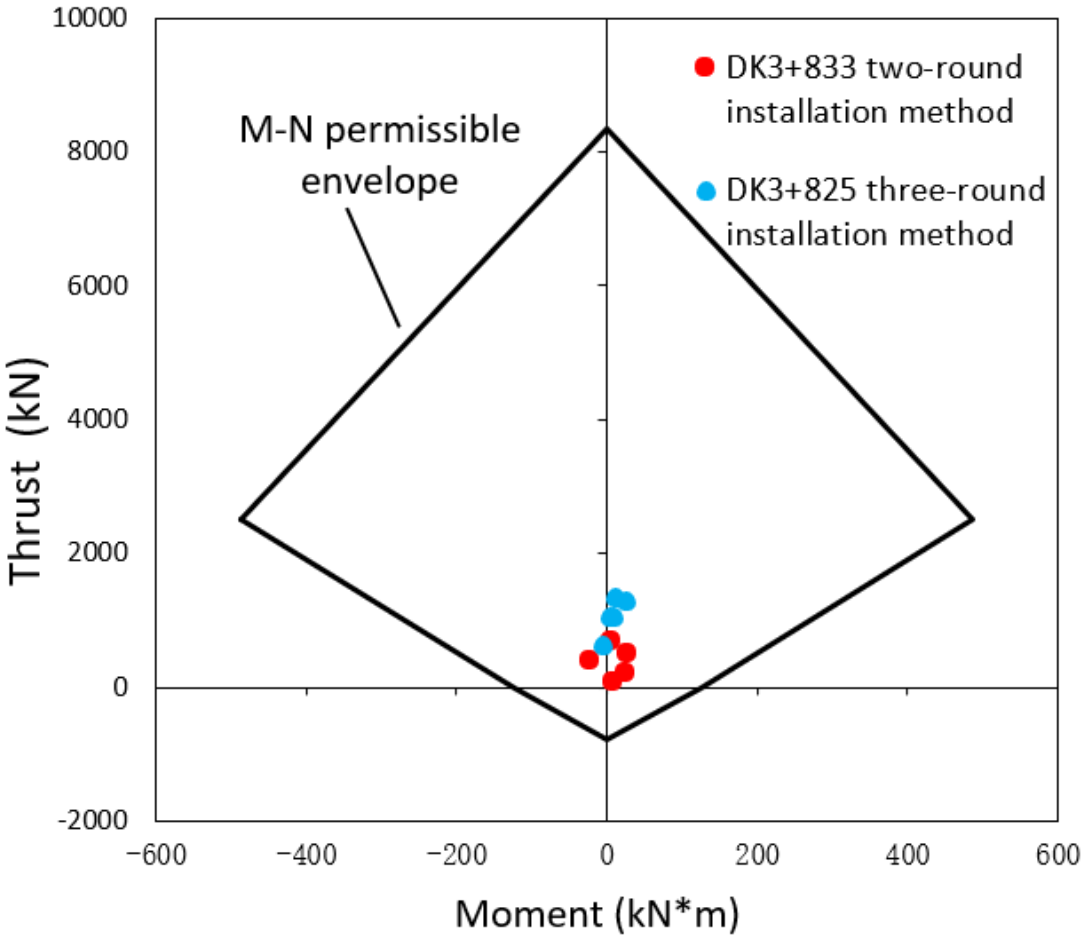

Fig.21 moment-thrust diagram for secondary lining internal forces

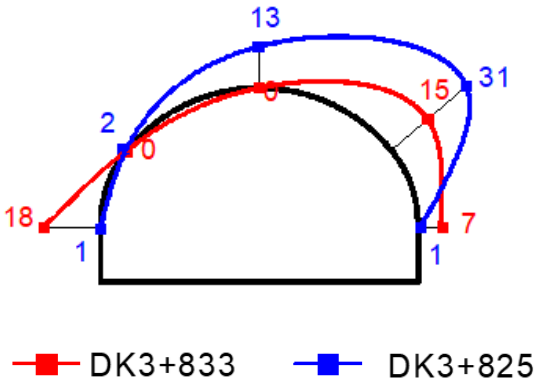

Figure 22 pressure on secondary lining /kPa (red line for two-round installation (DK3+833) and blue line for three-round installation (DK3+825))

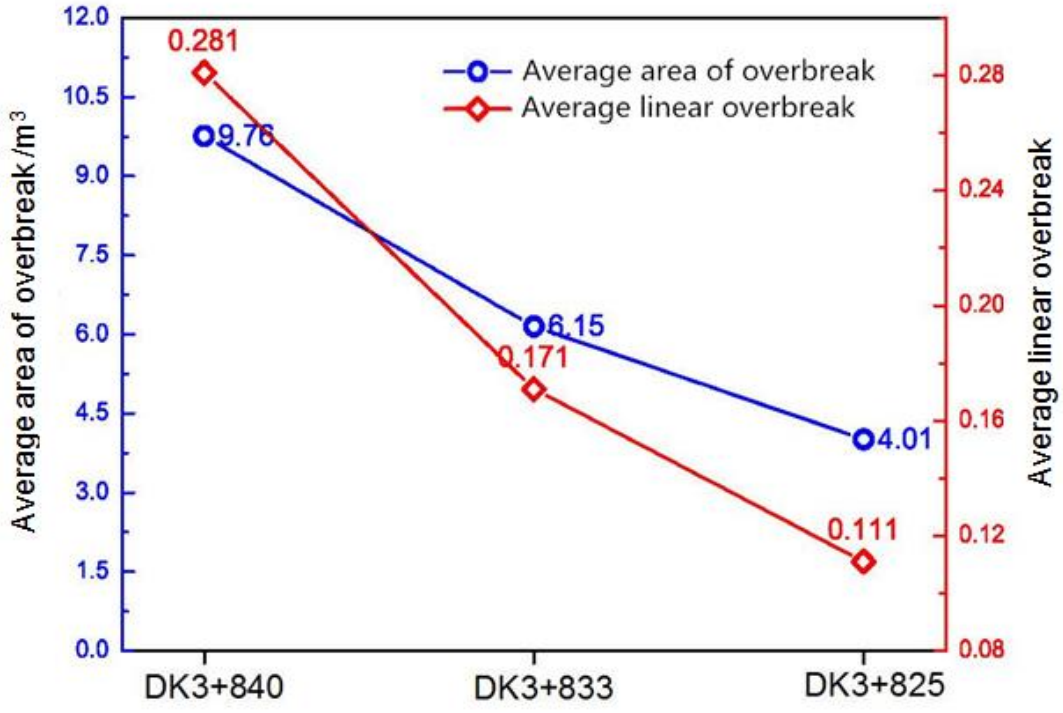

Fig.23 The relationship between over-excavation area and linear over-excavation

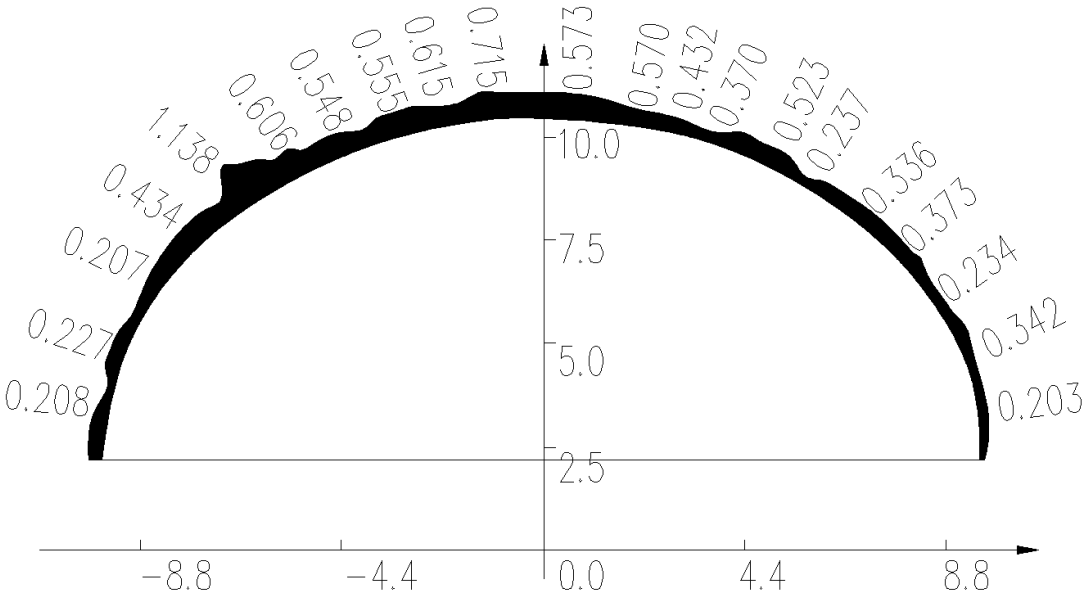

(a) Section 840 for one-round installation method

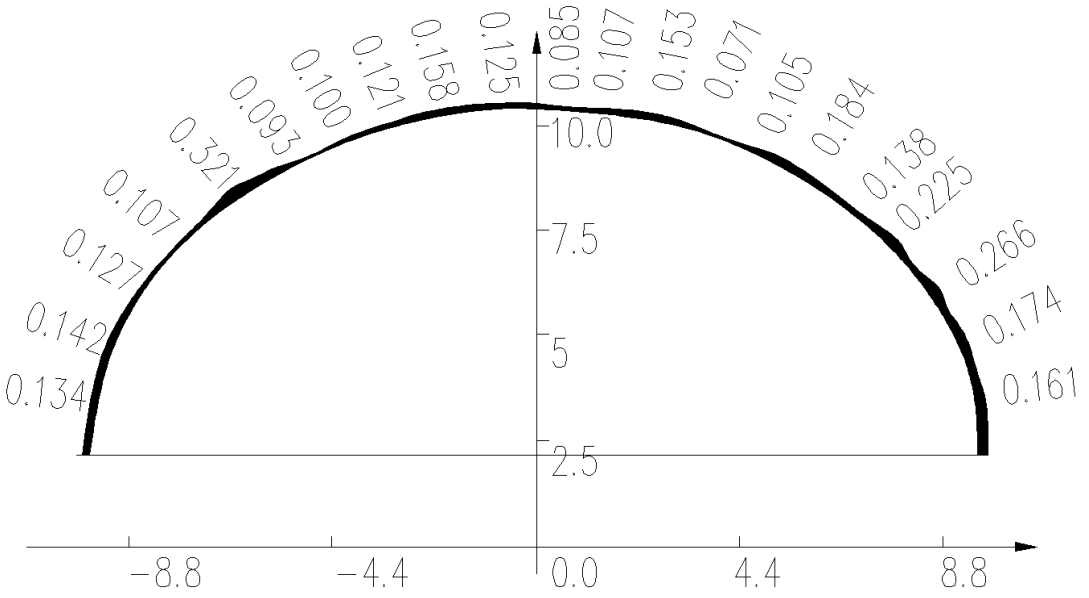

(b) Section 825 for three-round installation method

Fig.24 Tunnel circumference due to over-excavation (unit: m)

Table 1 Material properties of shotcrete, steel frame and reinforce concrete

Materials	Type	Strength
Steel frame	I-beam 16# 160mm x 88mm x 6.0mm	Q235: yield strength=235MPa
Shotcrete	C25	Design compressive strength = 11.9MPa, Design tensile strength = 1.27MPa
Concrete in secondary lining	C35	Design compressive strength = 16.7MPa, Design tensile strength = 1.57MP

Table 2 Sensor specifications and monitoring chainage

Monitoring chainage	Installation timing of initial ground support	Sensor specifications
DK3+840	One-round installation	pressure cell (range 0.6MPa; resolution ±0.001MPa; accuracy ≤1%F·S): pressure between surrounding rock and initial ground support; embedded strain gauge (range ±1500με; resolution 1με; accuracy ≤1%F·S): stress in shotcrete of initial ground support; strain gauge (range ±1200με; resolution 1με; accuracy ≤1%F·S): stress in steel frame of initial ground support
DK3+833	Two-round installation	
DK3+825	Three-round installation	
DK3+833	Two-round installation	pressure cell (range 0.6MPa; resolution ±0.001MPa; accuracy ≤1%F·S): pressure between initial ground support and secondary lining; embedded strain gauge (range ±1500με; resolution 1με; accuracy ≤1%F·S): stress in secondary concrete; strain gauge (range ±1200με; resolution 1με; accuracy ≤1%F·S): stress in steel bar of secondary lining
DK3+825	Three-round installation	

Table 3 Comparison of construction time duration of the three installation methods

Step	Description	Average time duration per 3.5m tunnel advance (min)		
		One-round installation	Two-round installation	Three-round installation
1	Surveying	40	30	30
2	Drilling preparation	20	20	20
3	Drilling of blastholes	70	50	50
4	Charging & blasting	90	60	50
5	Ventilation	30	30	30
6	Safety Provisions	240	180	260
7	Steel frame installation	200	170	170
8	Spraying Shotcrete	390	240	240
9	Total time duration	1080	780	850